REVIEW   **Open Access**

Preceding seismic activity and slow slip events in the source area of the 2011 Mw 9.0 Tohoku-Oki earthquake: a review

Akira Hasegawa[1*] and Keisuke Yoshida[2]

Abstract

The 2011 Tohoku-Oki earthquake ruptured a large area of the megathrust east of NE Japan. The earthquake's magnitude was 9.0, substantially larger than predicted. It is important to know what occurred in the source area prior to this great megathrust earthquake to improve understanding of the nucleation processes of large earthquakes and risk assessments in subduction zones. Seafloor observation data revealed the existence of two extremely large slip patches: one just updip of the mainshock hypocenter and the other 80–100 km to the north near the trench axis. For 70–90 years before 2003, M > 6 events and slips of M > c. 7 events on the megathrust occurred in the areas surrounding these two large slip patches. Seismic activity had increased since at least 2003 in the downdip portion of the source area of the Tohoku-Oki earthquake. In addition, long-term accelerated slow slip occurred in this downdip portion of the source area in the decades before the Tohoku-Oki earthquake. About 1 month before the earthquake, a slow slip event (SSE) took place at relatively shallow depths between the two large slip patches, accompanied by foreshock activity. Both the slow slip and foreshocks propagated from north to south toward the southern large slip patch. Two days before the earthquake, an M 7.3 foreshock and an associated postseismic slip began at relatively deep depths in the megathrust between the two large slip patches. In addition, a slow slip type event seems to have occurred approximately half a day after the M 7.3 foreshock near the mainshock hypocenter. This slow slip event and the foreshock activity again propagated from north to south toward the mainshock hypocenter. These long- and short-term preceding seismic and aseismic slip gradually reduced the interplate coupling, increased shear stresses at the two large slip patches (i.e., two strong asperity patches), and finally led to the rupture of the great Tohoku-Oki earthquake.

Keywords: 2011 Tohoku-Oki earthquake; Precursory seismic activity; Precursory SSEs; Foreshocks; Earthquake nucleation process

Introduction

The Mw 9.0 Tohoku-Oki earthquake on March 11, 2011, the largest earthquake in the modern history of Japan, occurred along the plate interface east of Tohoku, NE Japan. The rupture area was approximately 500 km long and 200 km wide (e.g., Japan Meteorological Agency, http://www.jma.go.jp/jma/indexe.html; Geospatial Information Authority of Japan, http://www.gsi.go.jp/ENGLISH/index.html), extending for about two thirds of the length of the megathrust zone east of the NE Japan arc. The earthquake caused severe damage in NE Japan. In particular,

the massive tsunami it generated caused many casualties along the Pacific coast, resulting in nearly 20,000 dead or missing individuals.

The 2011 Tohoku-Oki megathrust earthquake was an unprecedented great earthquake because of the amount and quality of observation data. It occurred in the most densely instrumented subduction zone in the world. Nationwide dense seismic and GPS networks, with a station separation of c. 20 km, were deployed on land in the Japanese islands after the 1995 M 7.3 Kobe earthquake. Seafloor geodetic monitoring systems with GPS-acoustic ranging were deployed on the landward slope of the major trenches. Particularly, prior to the Tohoku-Oki earthquake, intensified observations of the seafloor through seismic and geodetic monitoring, including ocean bottom

* Correspondence: hasegawa@aob.gp.tohoku.ac.jp
[1]Research Center for Prediction of Earthquakes and Volcanic Eruptions, Graduate School of Science, Tohoku University, Sendai 980-8578, Japan
Full list of author information is available at the end of the article

pressure (OBP) gauges, had been made in the area off Miyagi Prefecture, where an extremely large slip occurred in the Tohoku-Oki earthquake. This is because of the high probability of earthquake occurrence in this area as assessed by the Government's Headquarters for Earthquake Research Promotion (Earthquake Research Committee, Headquarters for Earthquake Research Promotion, http://www.jishin.go.jp/main/index-e.html), although the forecast itself, based mainly on records of previous large earthquakes, dramatically underestimated the magnitude of the 2011 event. The maximum forecast magnitude for this area was 8.2, much smaller than the Mw 9.0 event that actually occurred.

The abundant data collected can improve our understanding of this megathrust earthquake, including the rupture process, the large size of the generated tsunami, and why such a large magnitude (Mw 9.0) earthquake occurred in this subduction zone. Numerous papers have been published based on various analyses of these data. Several papers [1–7], including a review paper [8], report anomalous earthquake activities and/or slow slip events (SSEs) in the source area preceding the Tohoku-Oki earthquake. Some of the observational evidence in these reports was obtained from the intensified observations of the seafloor geodetic monitoring in the source area. It is particularly important to know the details of what occurred overall in the source area prior to this great megathrust earthquake, to improve our understanding of the stress accumulation and nucleation processes of large earthquakes and for seismic hazard assessments and mitigation in subduction zones. In this review, we focus on the activity of earthquakes and SSEs in the source area of the 2011 Tohoku-Oki earthquake in the pre-mainshock period and their relation to the mainshock rupture.

Review

Coseismic slip distribution: two large slip patches

Many researchers have studied the coseismic slip distribution and rupture process of the M 9.0 Tohoku-Oki megathrust earthquake by analyzing seismic, geodetic, and tsunami data. Slip distributions, estimated soon after this earthquake, can be classified into two groups: one having a large slip near the trench axis [9–13] and the other having a large slip near the mainshock hypocenter [14–18]. Subsequently, data from instruments installed at the sea bottom right above the source area were published, and these seafloor geodetic data provided clear evidence for a large slip in the near-trench area [19–21]. For example, GPS-acoustic ranging data show that the horizontal displacement at a site c. 50 km landward of the trench axis amounts to 31 m toward the ESE, in contrast to the maximum value of 5.3 m from onshore GPS data along the Pacific coast. Information on crustal

deformation was also provided by OBP gauges installed directly above the source area. Slip inversions including these seafloor data indicate an anomalously large slip in the near-trench area far off-Miyagi Prefecture, with the maximum slip exceeding c. 50 m.

The large near-trench slip seems to be consistent with the spatial distribution of aftershocks that occurred at the plate interface. After the Tohoku-Oki earthquake, interplate earthquakes did not occur in the mainshock large slip area but only in the surrounding areas [22]. Repeating earthquakes and smaller magnitude interplate earthquakes also did not occur in the large slip area after the Tohoku-Oki earthquake [23]. The stress field estimated from focal mechanisms also seems to support the large near-trench slip model. The stress field in the upper plate was completely transformed after the Tohoku-Oki earthquake. The minimum compressive stress axis became oriented in the direction of the large near-trench slip area, even near the trench axis, which is consistent with the static stress change by the large near-trench slip. This provides evidence for the large near-trench slip at shallow depths during the mainshock rupture [24].

Figure 1 shows coseismic slip distributions of the Tohoku-Oki earthquake estimated from joint inversions of onshore GPS and seafloor geodetic data (Fig. 1a–c) [3,5,25] or of onshore GPS, seafloor geodetic, and tsunami data (Fig. 1d) [26]. A zero slip boundary condition was not implemented at the trench in these inversions. As described above, all the slip models in the figure that include the seafloor geodetic data have a common feature: a large slip occurs in the shallow part of the plate interface near the trench axis. Looking at the models in more detail, another common feature exists: the large slip area is divided into two large slip patches separated by a zone of relatively low slip. One patch is located just updip of the mainshock hypocenter, and the other is located 80–100 km to the north of the first patch. The exception to this distribution is the model in Fig. 1a, in which the largest slip is located at the shallowest portion of the plate interface along the trench axis, although even in this model, relatively large slips are distributed at the same locations as the two large slip patches in the other models. The locations of the two large slip patches mentioned above are almost identical among the remaining three slip models (Fig. 1b–d), although slight differences are visible in the northern patch, which may be due to the spatial resolution of the inversions. Other common features exist for the three models: peak slip in the southern patch is larger than in the northern patch, and the peak slip in this primary patch occurs just updip of the mainshock hypocenter (70–90 km landward of the trench axis), in contrast to the northern secondary patch where the peak slip occurs near
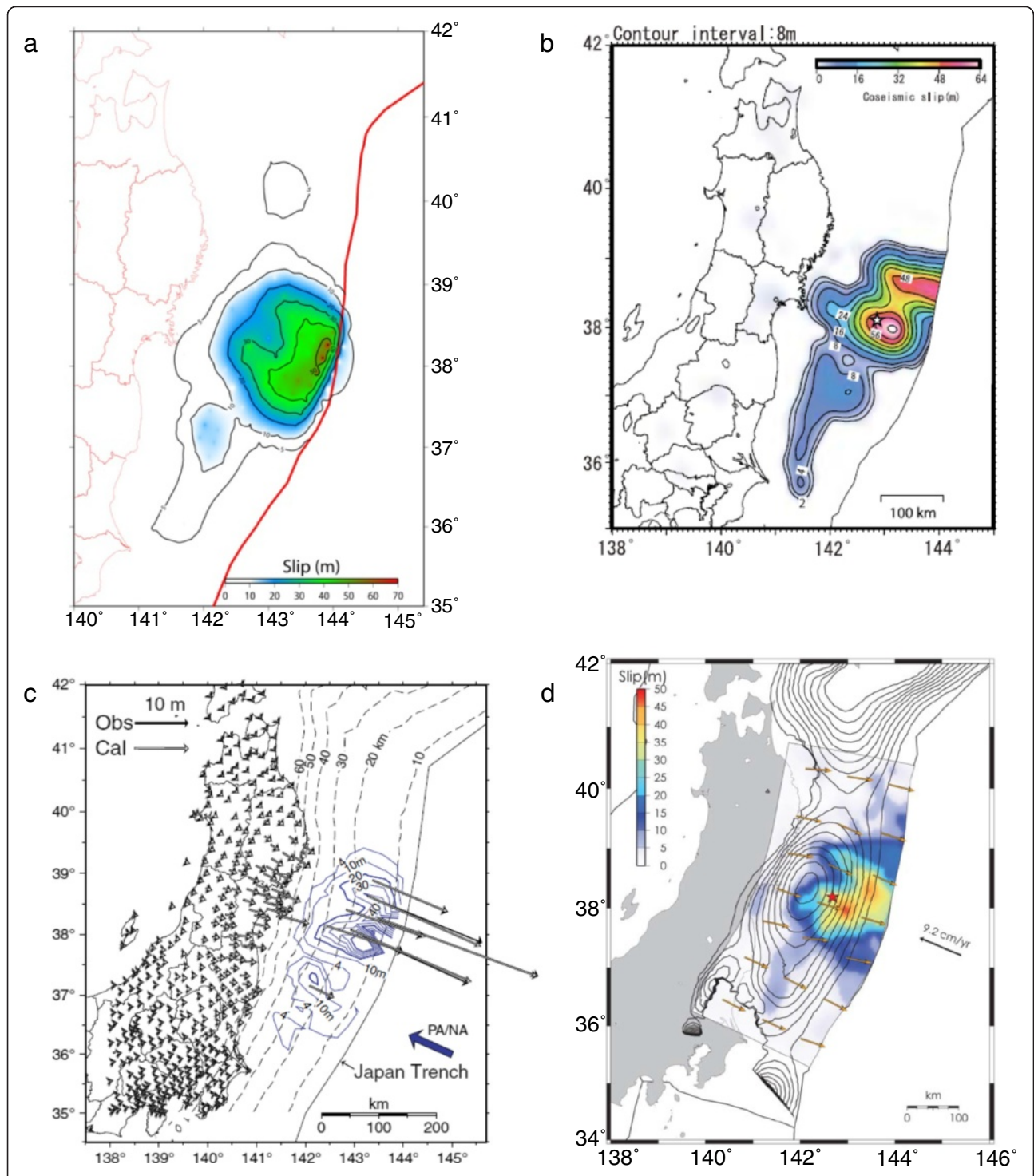
Fig. 1 Coeseismic slip distribution of the 2011 Tohoku-Oki earthquake estimated from inversions of data including seafloor geodetic data. Slip models by **a** Iinuma et al. [25] (contour interval: 10 m with 5-m contour line), **b** Ozawa et al. [3] (contour interval: 8 m with 2 m- and 4 m-contour lines), **c** Sato et al. [5] (contour interval: 10 m with 4-m contour line), and **d** Romano et al. [26]. In **d**, slip is shown by the *color scale*, and *thin black contours* indicate the interseismic coupling (from 10 % to 100 %, at 10 % intervals). The *star* represents the mainshock hypocenter

the trench axis and the large slip reaches the trench axis. Thus, the slip models in Fig. 1 are divided into two groups: one (group 1)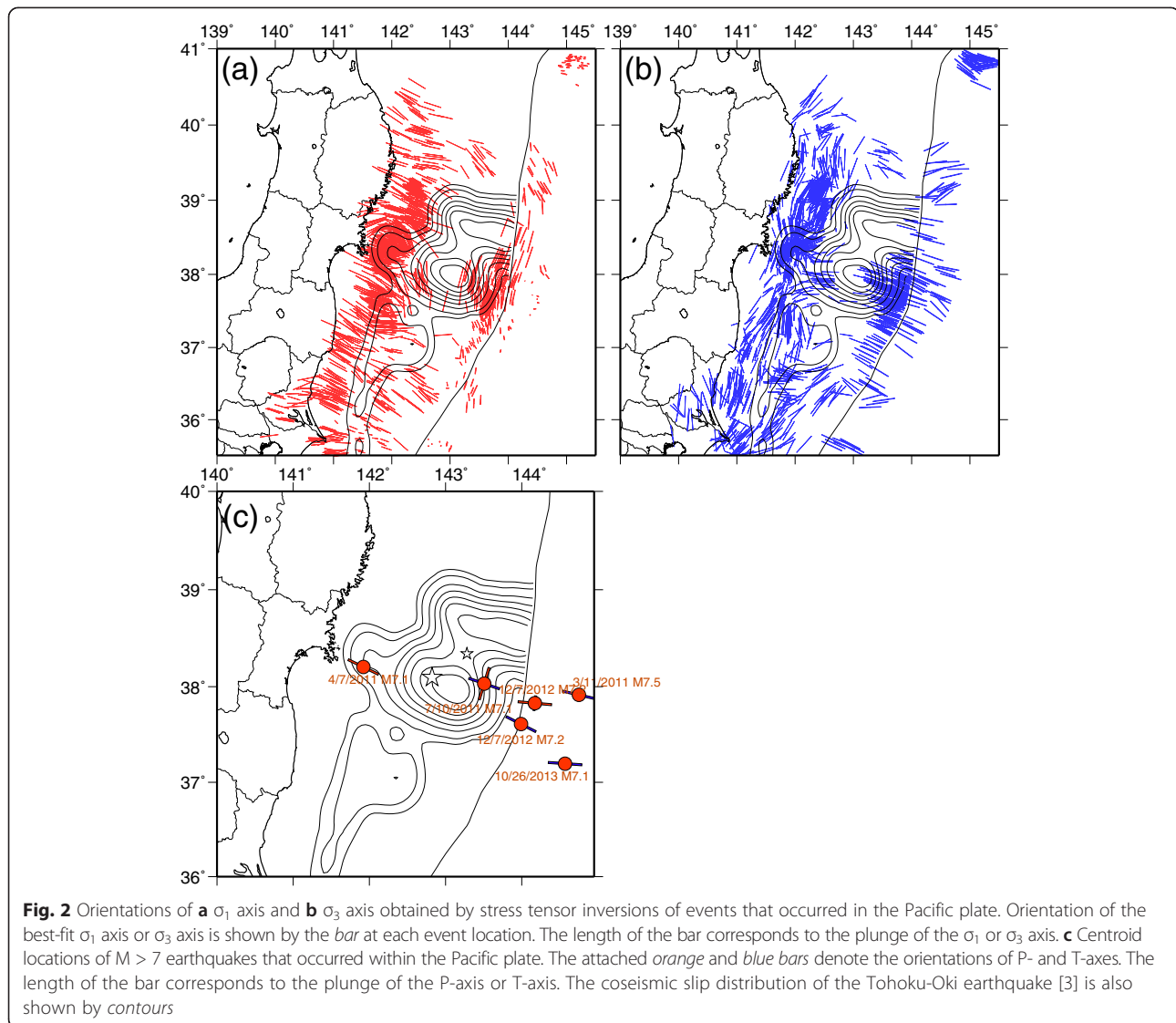 having the largest slip at the shallowest portion (Fig. 1a) and the other (group 2) having two large slip patches at the shallow plate interface (Fig. 1b–d).

Different inversion procedures and data are used among the slip models shown in Fig. 1 to estimate coseismic slip distribution. For example, the model shown in Fig. 1d did not involve a large upheaval at the station (TJT1) located above the large slip area c. 20 km landward of the trench axis. In this area, the easternmost portion of the upper plate is an accretionary prism, composed of extremely low rigidity materials, with a width of 25–30 km [27,28]. It is probable that an inelastic response was involved to some extent in the extremely large upheaval at that station, and so the data may not be appropriate for inclusion in the slip inversion, as noted by Romano et al. [26]. The dip angle of the assumed fault plane at the shallowest portion is also different among the slip models in Fig. 1, which strongly affects the estimated slip amount for this area. Thus, it is difficult to determine whether or not the largest slip actually occurred at the shallowest portion of the plate interface.

Here, we infer the slip distribution from a different set of data: spatial distribution of the principal stress orientations in the footwall after the Tohoku-Oki earthquake. We estimated the stress orientations in the Pacific plate by stress tensor inversions of focal mechanisms for events that occurred after the Tohoku-Oki earthquake. Focal mechanism data are from F-net CMT solutions determined by the National Research Institute for Earth Science and Disaster Prevention (NIED). We estimated the principal stress orientations in the vicinity of each focal mechanism as follows. First, we set the maximum range of the distance between the slave event and the master event (r). We then estimated principal stress orientations at the hypocenter of each focal mechanism (master event) by applying the stress tensor inversion code of Michael [29] to the data of all focal mechanisms (slave events) located within r kilometers if the number of such events was <25. If the total number of these events was >25, we used the 25 events closest to the master event. If there were <10 qualifying events, we did not estimate the principal stress orientations at that master event location. We took r to be 40 km in the horizontal direction and 25 km in the vertical direction. The orientations of the maximum and minimum principal stress axes in the Pacific plate are shown in Fig. 2a–b, respectively. The slip distribution of the Tohoku-Oki earthquake, estimated, for example, by Ozawa et al. [3], is also shown in the figure as representative of group 2. The figure shows that earthquakes that occurred in the footwall are concentrated just to the ESE and to the WNW of the southern primary large slip patch. Events just to the ESE of the patch have the maximum principal stress axes oriented trench-parallel and the minimum principal stress axes oriented trench-perpendicular. In contrast, events just to the WNW of the patch have the maximum principal stress axes oriented trench-perpendicular

and the minimum principal stress axes oriented trench-parallel. These stress orientations can be explained by the existence of the southern primary large slip patch in group 2 if these events, which occurred in the footwall after the mainshock, were triggered by the static stress change of the mainshock rupture. The model with the largest slip at the shallowest portion of the plate interface (group 1) cannot explain these stress orientations. A similar hypothesis was put forward by Chiba et al. [30], who investigated the stress field in the focal area of the Tohoku-Oki earthquake. They noted that the aftershock focal mechanism distribution in the footwall constrains the spatial distribution of the moment release of the Tohoku-Oki earthquake: the largest moment release is located just updip of the mainshock hypocenter rather than in the vicinity of the trench axis. This is consistent with the southern primary large slip patch commonly visible in the group 2 slip models. For the northern secondary patch, trench-parallel oriented maximum principal stress axes are not visible at locations landward of the trench axis, supporting the northern patch reaching the trench axis.

Large earthquakes that occurred in the footwall after the Tohoku-Oki earthquake also support the group 2 slip models. Five Mw > 7 earthquakes occurred around the source area in the Pacific plate after the Tohoku-Oki earthquake. One of these events, on December 7, 2012, was a doublet that occurred in the trench-outer rise region. An Mw 7.2 thrust event first ruptured at depths of 50–70 km, followed by an Mw 7.1–7.2 normal-faulting event about 27 km to the SSW at depths of 10–30 km [31]. The centroid locations of the doublet and the other four Mw > 7 events are shown in Fig. 2c. The orange and blue lines attached to the centroid locations are the orientations of the P- and T-axes. A comparison of the slip distribution with the locations of the Mw > 7 events clearly shows that these events occurred at locations where the shear stress increased favorably, triggering these large events by the static stress change of the mainshock rupture. Four Mw > 7 normal or strike-slip faulting events are located to the ESE of the southern primary large slip patch, with the T-axis oriented trench-perpendicular, and an Mw 7.1 thrust event near the coast line located to the WNW of the southern large slip patch with the P-axis oriented trench-perpendicular, which indicates that the increased stress due to the static stress change is large at these locations. The exception is the Mw 7.2 thrust event (50–70 km deep) that occurred as the first event of the doublet. This corresponds to the compressional deep trench-outer rise event [32] of the double-planed shallow seismic zone in the forearc region [33]. This event was located slightly further from the plate interface along which the mainshock slip occurred, and so the amplitude of the static stress change was relatively small at this event location. This event may have

Fig. 2 Orientations of **a** σ₁ axis and **b** σ₃ axis obtained by stress tensor inversions of events that occurred in the Pacific plate. Orientation of the best-fit σ₁ axis or σ₃ axis is shown by the *bar* at each event location. The length of the bar corresponds to the plunge of the σ₁ or σ₃ axis. **c** Centroid locations of M > 7 earthquakes that occurred within the Pacific plate. The attached *orange* and *blue bars* denote the orientations of P- and T-axes. The length of the bar corresponds to the plunge of the P-axis or T-axis. The coseismic slip distribution of the Tohoku-Oki earthquake [3] is also shown by *contours*

occurred because of the increased plate bending stress due to the mainshock rupture.

As described above, the slip distribution commonly visible in the group 2 slip models (Fig. 1b–d) is supported by the spatial distribution of the focal mechanisms of earthquakes that occurred in the Pacific plate after the Tohoku-Oki earthquake. On the other hand, the group 1 slip model (Fig. 1a) cannot explain the observed spatial distribution of the focal mechanisms and so will be excluded from the discussion hereafter.

Romano et al. [34] also estimated the coseismic slip distribution of the Tohoku-Oki earthquake by a joint inversion of onshore GPS, seafloor geodetic, and tsunami data, but their slip model is not included in this review. A three-dimensionally heterogeneous structure model was used in their inversion, and the depth-dependent rigidity

caused a slightly different spatial pattern of coseismic slip compared with that in Fig. 1d of Romano et al. [26], which was obtained under the assumption of homogeneous elastic constants. We cannot directly compare the slip model of Romano et al. [34] with slip distributions of preceding earthquakes and SSEs, since they were estimated under the assumption of homogeneous elastic constants. Therefore, we did not use the slip model of Romano et al. [34] but used slip models obtained using homogeneous elastic constants, as shown in Fig. 1. Moreover, if we convert the slip distribution in Romano et al. [34] to a moment release distribution, we would expect to obtain a similar spatial pattern to that in the slip model of Romano et al. [26], because the trend of large slips at shallower depths, compared with Romano et al. [26], is caused mainly by the depth-dependent rigidity.

Activity of earthquakes and SSEs preceding the Tohoku-Oki earthquake
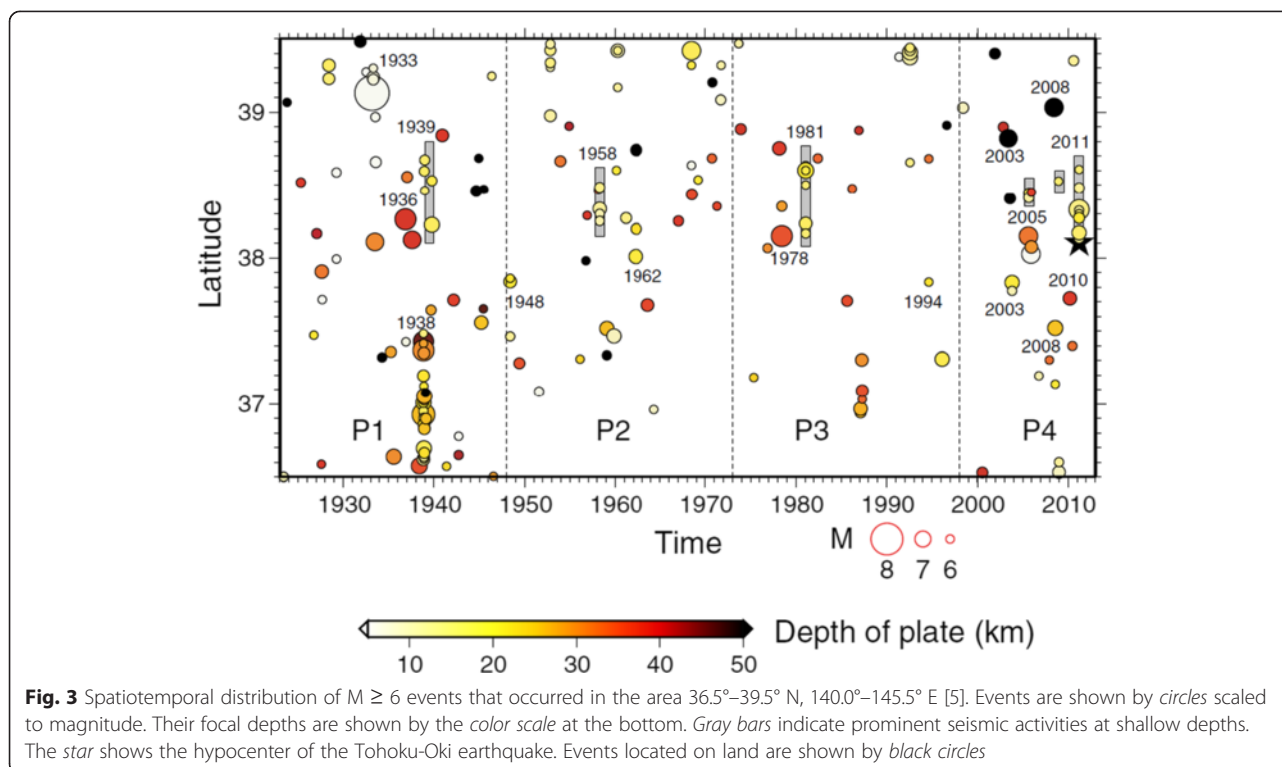
Seismic activity before 2003

The maximum slip at the two large slip patches is estimated to be 50–65 m (Fig. 1). The convergence rate in this subduction zone is 8–9 cm/year [35,36], and therefore such a large slip would take several hundred years to accumulate and the two large slip patches must have been locked for this period. Data observed by the instruments, however, date back to c. 100 years ago at the most. Sato et al. [5] investigated the preceding seismic activity in the source area of the Tohoku-Oki earthquake based on the Japan Meteorological Agency (JMA) catalog since 1923. They pointed out that large earthquakes with M > 6 that occurred during the c. 90 years preceding the Tohoku-Oki earthquake were located away from the two large slip patches. Figure 3 plots the latitudes of hypocenters against time for earthquakes with M > 6 that occurred beneath the Pacific Ocean in and around the source area before the Tohoku-Oki earthquake [5]. Several earthquake clusters stand out in the figure. They are the 1933 Sanriku earthquake that occurred in the outer rise region, the 1936 and 1978 off-Miyagi earthquakes that occurred in the deep thrust zone, the 1939, 1958, and 1981 far off-Miyagi earthquakes that occurred in the shallow thrust zone, and the 1938 off-Fukushima earthquakes that occurred in the shallow to deep thrust zone. Seismic activity in the source area had been relatively calm from the late 1930s, although the 1958, 1978,
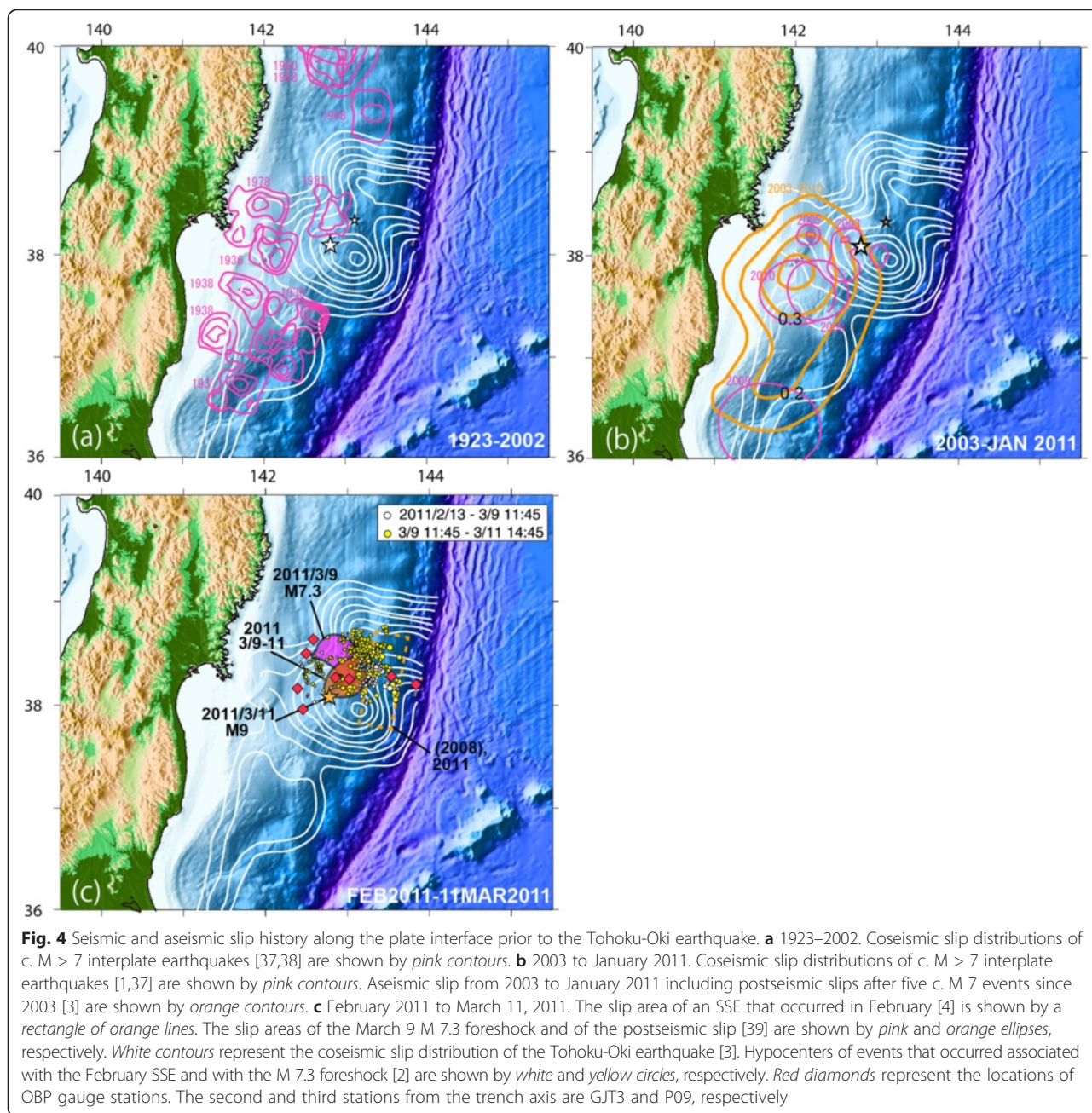
and 1981 events occurred in this area. This relatively calm period continued for c. 64 years until 2003.

Yamanaka and Kikuchi [37] and Murotani et al. [38] estimated slip distributions of c. M > 7 earthquakes that occurred on the megathrust east of NE Japan for the last c. 70 years by waveform inversions of nearfield strong motion records. The slip distributions of events obtained for this period are shown by the pink contours in Fig. 4a. A comparison with the slip distribution of the Tohoku-Oki earthquake (white contours) shows that the slips of c. M > 7 earthquakes, except the 1981 event, on the plate interface occurred in areas surrounding the large slip area of the Tohoku-Oki earthquake. Even for the 1981 event, the slip area is located in the region of relatively low slip between the two large slip patches described above. This indicates that the two large slip patches of the Tohoku-Oki earthquake were locked throughout this period, whereas the interplate coupling in the surrounding areas gradually reduced owing to the slips of these earthquakes.

Earthquake and SSE activity from 2003 to January 2011

From 2003, after the relatively calm period of c. 64 years, seismic activity in the source area of the Tohoku-Oki earthquake increased remarkably. In the c. 8 years preceding the Tohoku-Oki earthquake, six c. M 7 events occurred in the source area, in contrast to the lack of such events in the preceding c. 22 years. SSEs also began to occur on the plate interface after about 2003. These activities continued until the occurrence of the Tohoku-Oki earthquake.

Fig. 3 Spatiotemporal distribution of M ≥ 6 events that occurred in the area 36.5°–39.5° N, 140.0°–145.5° E [5]. Events are shown by *circles* scaled to magnitude. Their focal depths are shown by the *color scale* at the bottom. *Gray bars* indicate prominent seismic activities at shallow depths. The *star* shows the hypocenter of the Tohoku-Oki earthquake. Events located on land are shown by *black circles*

Fig. 4 Seismic and aseismic slip history along the plate interface prior to the Tohoku-Oki earthquake. **a** 1923–2002. Coseismic slip distributions of c. M > 7 interplate earthquakes [37,38] are shown by *pink contours*. **b** 2003 to January 2011. Coseismic slip distributions of c. M > 7 interplate earthquakes [1,37] are shown by *pink contours*. Aseismic slip from 2003 to January 2011 including postseismic slips after five c. M 7 events since 2003 [3] are shown by *orange contours*. **c** February 2011 to March 11, 2011. The slip area of an SSE that occurred in February [4] is shown by a *rectangle of orange lines*. The slip areas of the March 9 M 7.3 foreshock and of the postseismic slip [39] are shown by *pink* and *orange ellipses*, respectively. *White contours* represent the coseismic slip distribution of the Tohoku-Oki earthquake [3]. Hypocenters of events that occurred associated with the February SSE and with the M 7.3 foreshock [2] are shown by *white* and *yellow circles*, respectively. *Red diamonds* represent the locations of OBP gauge stations. The second and third stations from the trench axis are GJT3 and P09, respectively

Suito et al. [1] noticed that postseismic slips of these c. M 7 earthquakes were anomalously large. The geodetic inversions of terrestrial GPS data for five of these c. M 7 earthquakes showed that the total moment released by postseismic slips was much larger than that by coseismic slips. Time-dependent analysis of the GPS data for the period from 2003 to January 2011 by Ozawa et al. [3] showed a remarkable aseismic slip distributed over a broad region of the source area, as shown by orange contours in Fig. 4b. Time evolution of the moment released by this aseismic slip is shown in Fig. 5, which shows remarkable moment releases after the c. M 7

earthquakes (vertical dotted lines in the figure) lasting for a very long time. The total moment of this aseismic slip, which includes the postseismic slips of the five c. M 7 earthquakes, is c. Mw 7.7, about 2.5 times as large as that of the coseismic slips of these c. M 7 events. Figure 4b shows that these postseismic slips, together with coseismic slips, reduced the interplate coupling rate in the downdip portion (or SW portion) of the source area of the Tohoku-Oki earthquake after 2003. These aseismic and seismic slips seemed to partly invade the southern primary large slip patch. Namely, these preceding aseismic and seismic slips eroded the locked region, suggesting
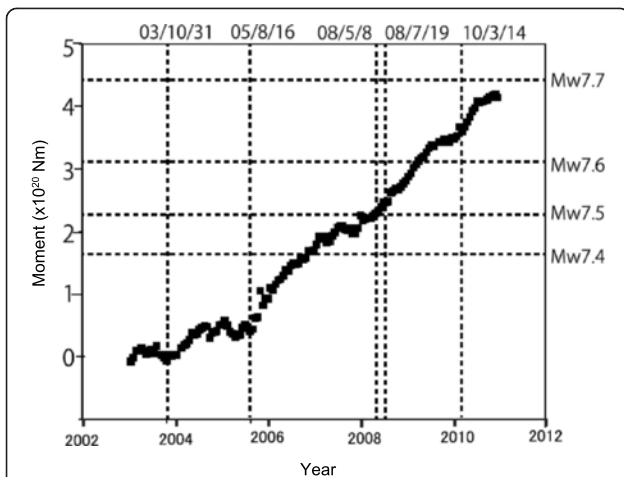
Fig. 5 Time evolution of the moment released by the aseismic slip on the megathrust east of central to south Tohoku during the period from 2003 to January 2011 [3]. *Vertical broken lines* show the times of the five c. M 7 interplate events since 2003

long-term precursory slip. The timing of the M 9.0 Tohoku-Oki earthquake appears to have been controlled by these multiple preceding slip events.

Mavrommatis et al. [6] modeled the GPS position time series in NE Japan as linear trends plus a constant acceleration, correcting for coseismic and postseismic effects from c. Mw > 6.5 earthquakes, for the period from 1996 to 2011, before the Tohoku-Oki earthquake (Fig. 6). They found spatially coherent and statistically significant long-term accelerations in the GPS time series at stations throughout Tohoku, NE Japan. The accelerations of GPS time series they observed at stations in northern Tohoku can be explained by the postseismic deformation from the pre-1996 subduction earthquake that was still decaying in the period after 1996. However, the accelerations of GPS time series they observed at stations in south-central Tohoku were not related to such postseismic effects. The long-term accelerations are associated with a decrease in the average contraction rate in the plate convergence direction and therefore can be explained by an increasing aseismic slip rate on the megathrust and/or by updip migration of aseismic slip from the deep plate interface in the decades preceding the Tohoku-Oki earthquake [6].
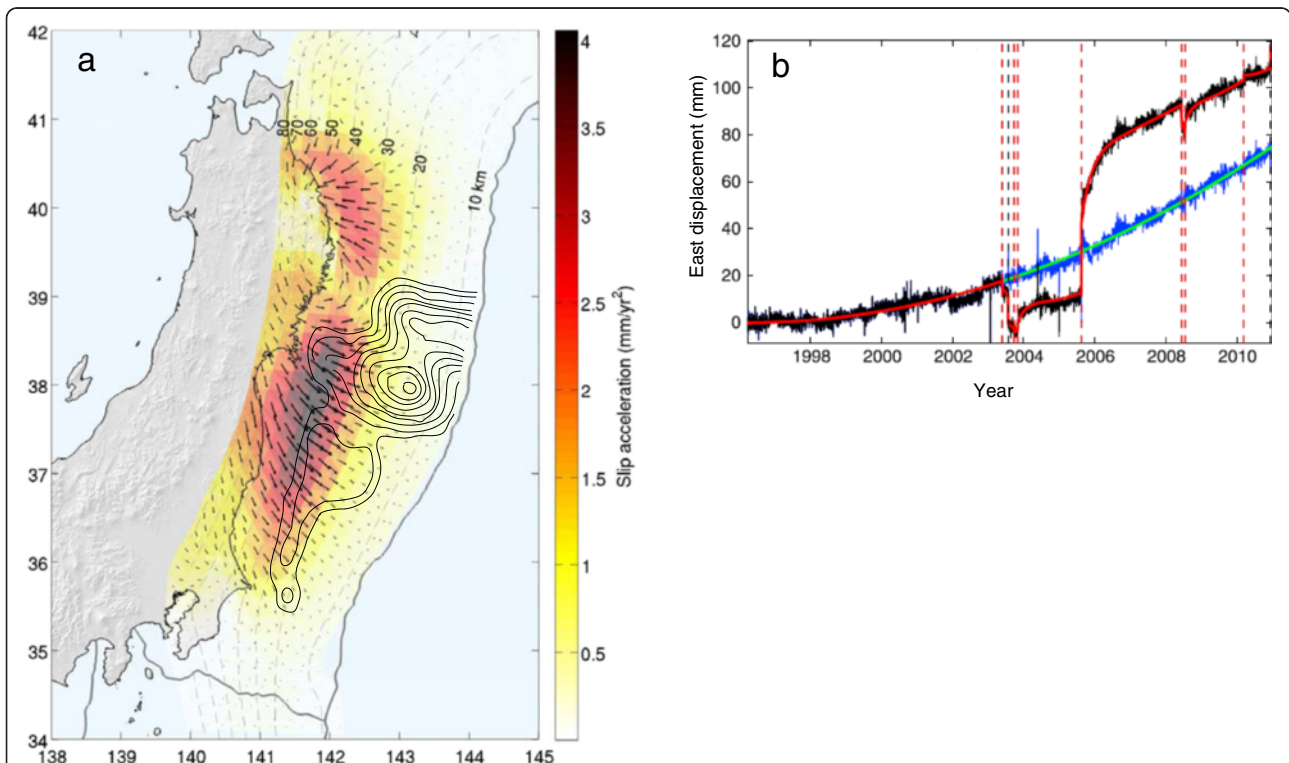
Fig. 6 Estimated decadal-scale slow slip acceleration prior to the Tohoku-Oki earthquake [6]. **a** Distribution of slow slip acceleration on the plate interface after inverting GPS position time series accelerations. *Colors* indicate the magnitude, and *vectors* indicate the direction of slow slip acceleration. *Black contours* represent the coseismic slip distribution of the Tohoku-Oki earthquake [3]. **b** GPS position time series at station 0036 (Onagawa). The *black curves* show the east component time series after removing common-mode errors, the *red curves* show postseismic transient model fits, and the *blue* and *green curves* show fits obtained after removing offsets and postseismic transients, respectively. *Vertical broken lines* mark the times of detected antenna offsets (*black*) and earthquakes (*red*). Initial linear trends have been removed

Yokota and Koketsu [7] also obtained tectonic deformations at GPS stations in NE Japan for the period preceding the Tohoku-Oki earthquake by removing the coseismic and postseismic slips of nearby Mw 6–8 earthquakes. They found a similar long-term transient, which is probably identical to that found by Mavrommatis et al. [6]. The slip area of the long-term transient they estimated on the plate interface is almost consistent with that shown in Fig. 6a.

The area of the postseismic slip estimated by Ozawa et al. [3], which is shown in Fig. 4b, is also almost identical to the slip area of the long-term transient estimated by Mavrommatis et al. [6], as shown in Fig. 6a. This indicates that the anomalously large postseismic slips of the c. M 7 earthquakes reported by Suito et al. [1] are explained by the fact that this long-term transient on the plate interface was also included in their inversions of postseismic slips of the c. M 7 earthquakes. Not only coseismic and postseismic slips of the c. M 7 events but also an accelerated aseismic slip occurred for >10 years before the Tohoku-Oki earthquake in the downdip portion (or SW portion) of the source area. This long-term precursory aseismic slip eroded the locked region composed of the two large slip patches.

Foreshock and SSE activity just before the mainshock

About 1 month before the Tohoku-Oki earthquake, foreshock and SSE activity began in close proximity to the two large slip patches.

OBP gauges installed directly above the source area detected an SSE that occurred in February 2011, just before the 2011 Tohoku-Oki earthquake [4]. This SSE took place at a relatively shallow depth between the two large slip patches, as shown in Fig. 4c by a rectangle of red broken lines. It lasted for c. 1 month, reaching c. Mw 7.0. This quasi-static slip propagated from north to south toward the southern large slip patch. Associated with this SSE, earthquake activity also began. Based on the waveform correlation method using template earthquakes located by the JMA, Kato et al. [2] identified a distinct foreshock sequence associated with the SSE, migrating toward the southern large slip patch (white circles in Fig. 4c). Figure 7 shows a space-time plot of the earthquakes, showing the propagation of hypocenters from north to south toward the southern primary large slip patch at a speed of 2 km/day for the first c. 6 days and of 5 km/day for the latter 5 days or so. The northern and southern edges of the estimated slip area of the SSE are not well constrained because of poor OBP station coverage in this
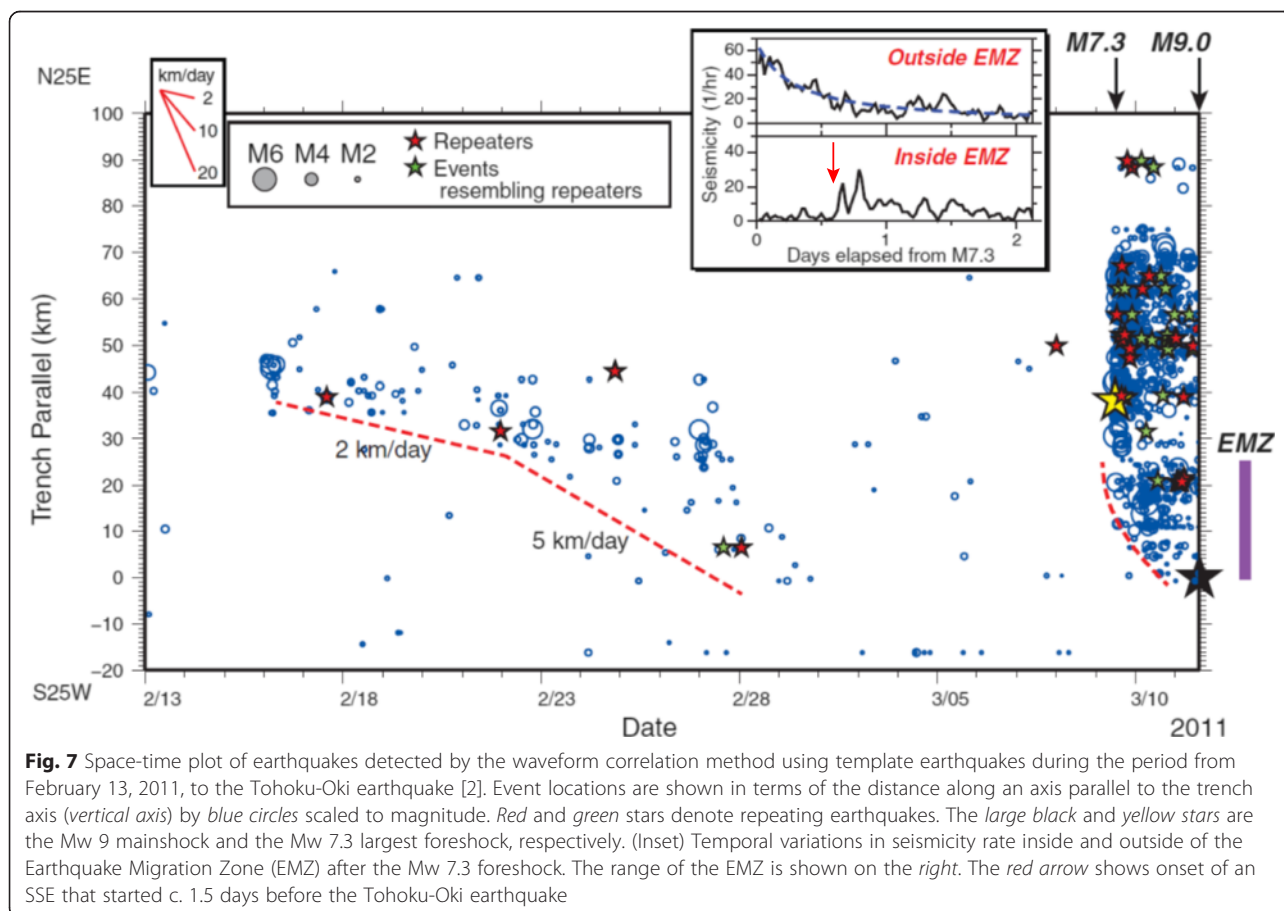

Fig. 7 Space-time plot of earthquakes detected by the waveform correlation method using template earthquakes during the period from February 13, 2011, to the Tohoku-Oki earthquake [2]. Event locations are shown in terms of the distance along an axis parallel to the trench axis (*vertical axis*) by *blue circles* scaled to magnitude. *Red* and *green stars* denote repeating earthquakes. The *large black* and *yellow stars* are the Mw 9 mainshock and the Mw 7.3 largest foreshock, respectively. (Inset) Temporal variations in seismicity rate inside and outside of the Earthquake Migration Zone (EMZ) after the Mw 7.3 foreshock. The range of the EMZ is shown on the *right*. The *red arrow* shows onset of an SSE that started c. 1.5 days before the Tohoku-Oki earthquake

area (red diamonds in Fig. 4c). Therefore, the length of the slip area might be slightly shorter than that shown in Fig. 4c; the N–S extent of the hypocenter distribution for the corresponding foreshocks (white circles) estimated by Kato et al. [2] is slightly shorter than the slip area of the SSE (a rectangle of red broken lines). Thus, the slip area of the SSE is probably located in the area between the two large slip patches. A similar type of SSE was also detected by OBP gauges [4]. This similar SSE occurred over period of a week in November 2008 at the same location on the plate interface, reaching c. Mw 6.8.

On March 9, 2011, two days before the earthquake, an M 7.3 foreshock occurred in the vicinity of the hypocenter of the Tohoku-Oki earthquake. The slip area of this M 7.3 event, estimated from onshore GPS and OBP gauge data [39], is shown by a pink ellipse in Fig. 4c. The figure shows that it was again located at the plate interface between the two large slip patches but relatively deep compared with the SSE that had begun about 1 month earlier (the rectangle of red broken lines in Fig. 4c). This M 7.3 foreshock was accompanied by after-shock activity and postseismic slip. Hypocenters of the aftershocks are shown by yellow circles in Fig. 4c. The postseismic slip, again estimated from onshore GPS and OBP gauge data [39], is shown by an orange ellipse in Fig. 4c. The postseismic slip broke an area just updip of the coseismic slip area and propagated from north to south toward the hypocenter of the Tohoku-Oki earthquake. The estimation using the waveform correlation method by Kato et al. [2] showed that aftershock activity

of the M 7.3 foreshock also propagated toward the hypocenter of the Tohoku-Oki earthquake at a speed of c. 10 km/day (Fig. 7). The postseismic slip lasted for more than 2 days, reaching c. Mw 6.8 [39], and finally leading to the rupture of the Tohoku-Oki earthquake.

As described above, for a time scale of decades before the Tohoku-Oki earthquake, there occurred a long-term transient (i.e., the accelerated slow slip) in the downdip portion of the source area on the megathrust (Fig. 6b) [6]. However, for a time scale of approximately 1 day before the Tohoku-Oki earthquake, no significant accelerating preslip was detected. Hino et al. [40] carefully examined OBP gauge records obtained near the mainshock hypocenter (locations of OBP stations are shown by red diamonds in Fig. 4c). Nontectonic coherent fluctuations visible at all the stations were removed by subtracting the first principal component of the principal component analysis of the records. After removing these oceanographic effects, they obtained a time series of seafloor vertical deformation in the area near the mainshock hypocenter with a noise level of 2–4 cm. The obtained time series is shown in Fig. 8. The postseismic deformation that began after the M 7.3 foreshock and decayed as shown by log-t fitting of the postseismic slip (dotted curves) is apparent in the figure [40]. Looking at the figure in more detail, however, a component exists that does not obey the log-t curve but shows the onsets of pressure changes delayed by about half a day as shown by a red arrow. Delayed onset of pressure increases is particularly noticeable at stations P09 and GJT3, which suggests
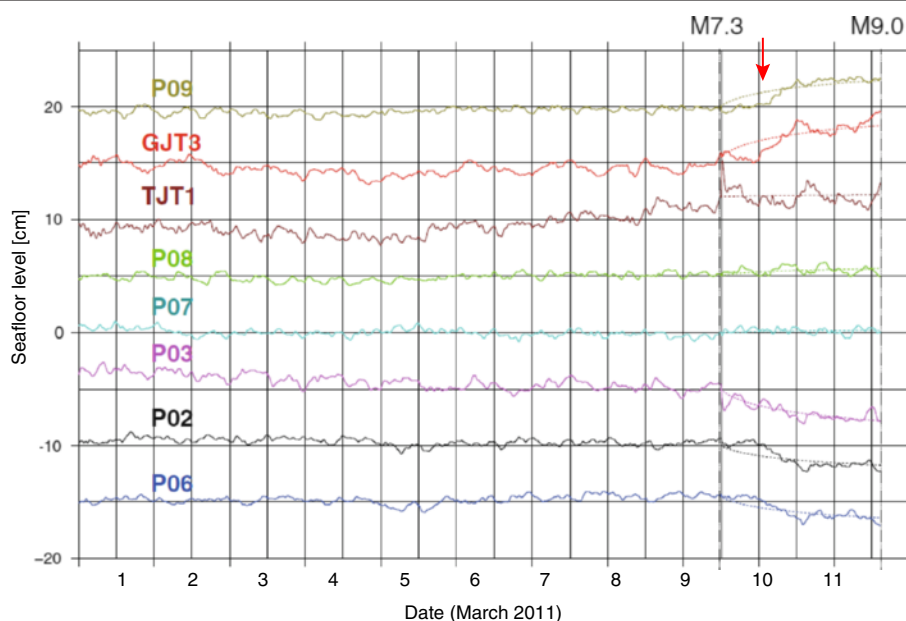

Fig. 8 Time series of seafloor level variations at 8 OBP gauge stations for 11 days prior to the Tohoku-Oki earthquake after reducing nontectonic fluctuations [40]. *Dashed curves* show temporal variations due to the postseismic slip after the Mw 7.3 foreshock, obtained by log-t fitting to the observations. The *red arrow* shows onset of an SSE that started c. 1.5 days before the Tohoku-Oki earthquake

that a slow slip type event, rather than an afterslip, occurred and is included in the observed OBP gauge records. The south group of the seismic activity after the M 7.3 foreshock (inside "Earthquake Migration Zone (EMZ)") also has a peak delayed by approximately half a day as shown by a red arrow in the inset at the top right in Fig. 7 [2]. This seismic activity in the south that migrated toward the mainshock hypocenter might have occurred in association with the slow slip type event mentioned above. Thus, although no significant accelerating preslip was detected, it seems that, in addition to the afterslip of the M 7.3 foreshock, there occurred a slow slip event that started c. 1.5 days before the Tohoku-Oki mainshock and migrated toward the mainshock hypocenter.

The history of the seismic and quasi-static slips along the plate interface described above and the slip distribution of the Tohoku-Oki earthquake, as summarized in Fig. 4, suggest the existence of persistent locked areas that probably correspond to strong asperity patches. Seismic and aseismic slips on the megathrust surrounding these two strong asperity patches (i.e., the two large slip patches) increased shear stress and finally quasi-static slips propagated toward the initial rupture point of the Tohoku-Oki earthquake within the southern strong patch, triggering the great M 9.0 megathrust earthquake. This is what actually occurred in the source area prior to this great megathrust earthquake, which is important in relation to understanding the nucleation processes of great megathrust earthquakes.

Discussion

The preceding slip history in the source area on the megathrust and the coseimic slip distribution of the Tohoku-Oki earthquake suggest the existence of a persistent locked area. The slip amount of 50–65 m indicates that this area had been locked for several hundred years. The core of this persistent locked area is thought to be composed of two strong asperity patches existing in the shallow portion of the megathrust zone. It is important to understand what causes such strong asperity patches on the plate interface.

Structural heterogeneities in the megathrust zone probably play an important role in the formation of such strong asperity patches. Zhao et al. [41] obtained a 3D seismic velocity structure in and around the source area of the Tohoku-Oki earthquake using local P-, S-, and sP-wave arrival times. Figure 9 shows the obtained P-wave velocity perturbations along the plate interface, together with the slip distribution of the Tohoku-Oki earthquake. The two large slip areas are located at P-wave high-velocity zones on the plate interface, whereas the areas to the north and south are characterized by P-wave low velocities. Similar correspondences between large slip areas (asperities) and P-wave high-velocity regions on the fault
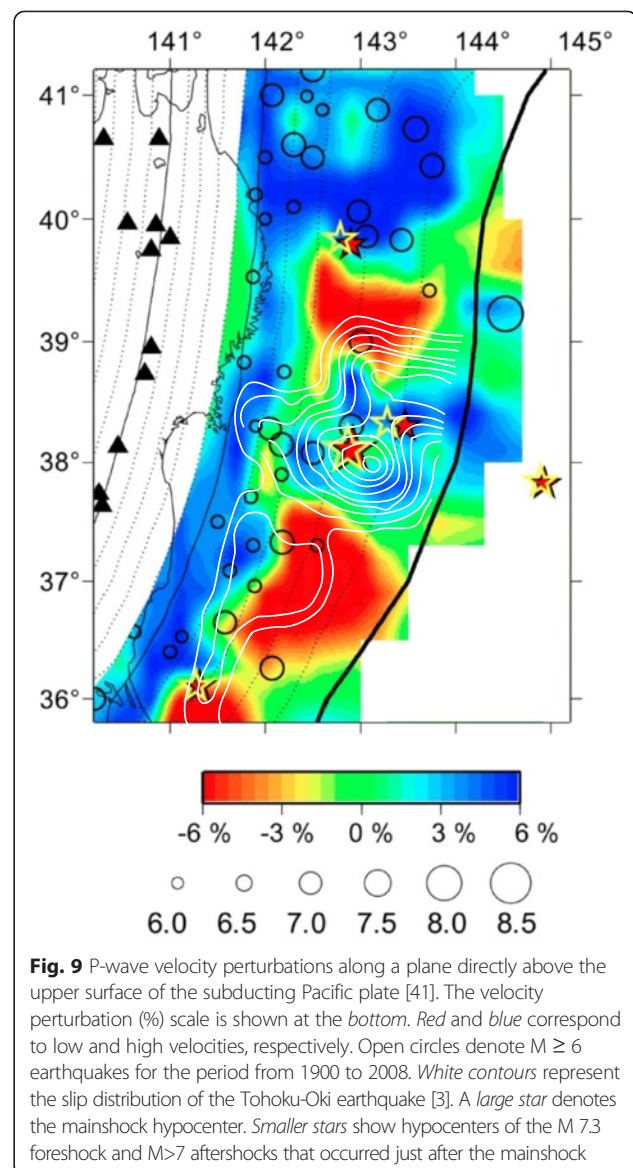

Fig. 9 P-wave velocity perturbations along a plane directly above the upper surface of the subducting Pacific plate [41]. The velocity perturbation (%) scale is shown at the *bottom*. *Red* and *blue* correspond to low and high velocities, respectively. Open circles denote M ≥ 6 earthquakes for the period from 1900 to 2008. *White contours* represent the slip distribution of the Tohoku-Oki earthquake [3]. A *large star* denotes the mainshock hypocenter. *Smaller stars* show hypocenters of the M 7.3 foreshock and M>7 aftershocks that occurred just after the mainshock

have been found for some of shallow inland earthquakes [42–44]. For the present megathrust earthquake, Zhao et al. [41] pointed out that the P-wave high-velocity patches in the megathrust zone may result from subducted seamounts or other topographic highs or compositional changes on the seafloor of the Pacific plate that become strong asperities where the upper and lower plates are strongly coupled. In contrast, the P-wave low-velocity areas in the megathrust zone may contain subducted sediments and fluids that cause the upper and lower plates to become weakly coupled or even decoupled.

A potential problem with this interpretation is the spatial resolution of the obtained P-wave velocity image. Arrival time data used in the tomographic inversions were obtained at routine seismic stations on land. A dense temporary OBS network was deployed after the Tohoku-Oki

earthquake above the large slip area. However, the result from Zhao et al. [41] cannot be confirmed from the tomographic image obtained using data from this network [45]. This is because the spatial extent of the OBS network was too small for confirmation; only the southern asperity patch was covered by the network. Further investigations of seismic tomography with higher spatial resolutions are required, based on a dense OBS network covering a broader area that includes the two strong asperity patches.

Conclusions

We have reviewed the activity of earthquakes and SSEs in the source area prior to the Tohoku-Oki earthquake. Seafloor observation data from directly above the large slip area of this event played an important role in constraining the coseismic slip distribution of the mainshock, showing the existence of two extremely large slip patches: one just updip of the mainshock hypocenter, 60–80 km landward of the trench axis, and the other 80–100 km to the north, near the trench axis. For c. 90 years before the Tohoku-Oki earthquake, M > 6 earthquakes occurred away from the two large slip patches. For c. 70 years, until 2003, slips of c. M > 7 earthquakes on the megathrust occurred in the areas surrounding the two large slip patches. Seismic and SSE activity increased after 2003. Six c. M 7 events occurred for 8 years from 2003 to 2010 in contrast to a complete absence of c. M 7 events for the preceding c. 22 years. These events occurred in the downdip portion of the source area of the Tohoku-Oki earthquake. Additionally, in this downdip portion of the source area, an increasing slip rate on the megathrust and/or updip migration of deep aseismic slip was observed in the decades before the Tohoku-Oki earthquake. These long-term precursory seismic and aseismic slips reduced the interplate coupling, partly eroding the locked region composed of the two large slip patches. About 1 month before the earthquake, an SSE took place at a relatively shallow depth between the two large slip patches. Associated with this SSE, foreshocks also began. Both slow slip and foreshock activity propagated from north to south toward the southern asperity patch. Two days before the earthquake, an M 7.3 foreshock occurred in the vicinity of the hypocenter of the Tohoku-Oki earthquake, again in the area between the two asperity patches but relatively deep compared with the SSE that had begun about 1 month earlier. This foreshock was accompanied by aftershock activity and postseismic slip located in the updip area between the two strong asperity patches. In addition, a slow slip event began c. 1.5 days before the Tohoku-Oki mainshock. This slow slip event and foreshock activity again propagated from north to south toward the mainshock hypocenter, the initial rupture point of the Tohoku-Oki earthquake, leading to the final rupture of the great megathrust earthquake.

Author details
[1]Research Center for Prediction of Earthquakes and Volcanic Eruptions, Graduate School of Science, Tohoku University, Sendai 980-8578, Japan. [2]Now at National Research Institute for Earth Science and Disaster Prevention, 3-1 Tennodai, Tsukuba 305-0006, Ibaraki, Japan.

References
1. Suito H, Nishimura T, Tobita M, Imakiire T, Ozawa S (2011) Interplate fault slip along the Japan Trench before the occurrence of the 2011 off the Pacific coast of Tohoku earthquake as inferred from GPS data. Earth Planets Space 63(7):615–619. doi:10.5047/eps.2011.06.053
2. Kato A, Obara K, Igarashi T, Tsuruoka H, Nakagawa S, Hirata N (2012) Propagation of slow slip leading up to the 2011 Mw 9.0 Tohoku-Oki earthquake. Science 335(2):705–708
3. Ozawa S, Nishimura T, Munekane H, Suito H, Kobayashi T, Tobita M, Imakiire T (2012) Preceding, coseismic, and postseismic slips of the 2011 Tohoku earthquake Japan. J Geophys Res 117(B7):B07404. doi:10.1029/2011JB009120
4. Ito Y, Hino R, Kido M, Fujimoto H, Osada Y, Inazu D, Ohta Y, Iinuma T, Ohzono M, Miura S, Mishina M, Suzuki K, Tsuji T, Ashi J (2013) Episodic slow slip events in the Japan subduction zone before the 2011 Tohoku-Oki earthquake. Tectonophysics 600:14–26. doi:10.1016/j.tecto.2012.08.022
5. Sato T, Hiratsuka S, Mori J (2013) Precursory seismic activity surrounding the high-slip patches of the 2011 Mw 9.0 Tohoku-Oki earthquake. Bull Seism Soc Am 106(6):3104–3114. doi:10.1785/0120130042
6. Mavrommatis AP, Segall P, Johnson KM (2014) A decadal-scale deformation transient prior to the 2011 Mw 9.0 Tohoku-Oki earthquake. Geophys Res Lett. 41. doi:10.1002/2014GL060139.
7. Yokota Y, Koketsu K (2015) A very long-term transient event preceding the 2011 Tohoku earthquake. Nature Comm 6:5934. doi:10.1038/ncomms6934, www.nature.com/naturecommunications
8. Kato A (2014) Slow slip transients before the 2011 Tohoku-Oki earthquake. J Disast Res 9:311–316
9. Fujii Y, Satake K, Sakai S, Shinohara M, Kanazawa T (2011) Tsunami source of the 2011 off the Pacific coast of Tohoku earthquake. Earth Planets Space 63:815–820
10. Lay T, Ammon CJ, Kanamori H, Xue L, Kim MJ (2011) Possible large near-trench slip during the 2011 Mw 9.0 off the Pacific coast of Tohoku earthquake. Earth Planets Space 63:687–692
11. Ide S, Baltay A, Beroza GC (2011) Shallow dynamic overshoot and energetic deep rupture in the 2011 Mw 9.0 Tohoku-Oki earthquake. Science 332:1426–1429
12. Yagi Y, Fukahata Y (2011) Rupture process of the 2011 Tohoku-Oki earthquake and absolute elastic strain release. Geophys Res Lett 38, L19307. doi:10.1029/2011GL048701
13. Koketsu K, Yokota Y, Nishimura N, Yagi Y, Miyazaki S, Satake K, Fujii Y, Miyake H, Sakai S, Yamanaka Y, Okada T (2011) A unified source model for the 2011 Tohoku earthquake. Earth Planet Sci Lett 310(3–4):480–487. doi:10.1016/j.epsl.2011.09.009
14. Simons M, Minson SE, Sladen A, Ortega F, Jiang J, Owen SE, Meng L, Ampuero J-P, Wei S, Chu R, Helmberger DV, Kanamori H, Hetland E, Moore AW, Webb FH (2011) The 2011 magnitude 9.0 Tohoku-Oki earthquake: Mosaicking the megathrust from seconds to centuries. Science 332(6036):1421–1425. doi:10.1126/science.1206731

15. Koper KD, Hutko AR, Lay T, Ammon CJ, Kanamori H (2011a) Frequency-dependent rupture process of the 2011 Mw 9.0 Tohoku earthquake: comparison of short-period P wave backprojection images and broadband seismic rupture models. Earth Planets Space 63(7):599–602. doi:10.5047/eps.2011.05.026

16. Ozawa S, Nishimura T, Suito H, Kobayashi T, Tobita M, Imakiire T (2011) Coseismic and postseismic slip of the 2011 magnitude-nine Tohoku-Oki earthquake. Nature 475:373–376. doi:10.1038/nature10227

17. Iinuma T, Ohzono M, Ohta Y, Miura S (2011) Coseismic slip distribution of the 2011 off the Pacific coast of Tohoku Earthquake (*M* 9.0) estimated based on GPS data—was the asperity in Miyagi-Oki ruptured? Earth Planets Space 63:643–648

18. Saito T, Ito Y, Inazu D, Hino R (2011) Tsunami source of the 2011 Tohoku-Oki earthquake, Japan: inversion analysis based on dispersive tsunami simulations. Geophys Res Lett 38:L00G19. doi:10.1029/2011GL049089

19. Sato M, Ishikawa T, Ujihara N, Yoshida S, Fujita M, Mochizuki M, Asada A (2011) Displacement above the hypocenter of the 2011 Tohoku-Oki earthquake. Science 332:1395

20. Kido M, Osada Y, Fujimoto H, Hino R, Ito Y (2011) Trench-normal variation in observed seafloor displacements associated with the 2011 Tohoku-Oki earthquake. Geophys Res Lett 38:L24303. doi:10.1029/2011GL050057

21. Ito Y, Tsuji T, Osada T, Kido M, Inazu D, Hayashi Y, Tsushima H, Hino R, Fujimoto H (2011) Frontal wedge deformation near the source region of the 2011 Tohoku-Oki earthquake. Geophys Res Lett 38:L00G05, 10.1029/2011GL048355

22. Asano Y, Saito T, Ito Y, Shiomi K, Hirose H, Matsumoto T, Aoi S, Hori S, Sekiguchi S (2011) Spatial distribution and focal mechanisms of aftershocks of the 2011 off the Pacific Coast of Tohoku earthquake. Earth Planets Space 63:669–673, http://dx.doi.org/10.5047/eps.2011.06.016

23. Uchida N, Matsuzawa T (2013) Pre- and postseismic slow slip surrounding the 2011 Tohoku-Oki earthquake rupture, Earth Planet. Sci Lett 374:81–91. doi:10.1016/j.epsl.2013.05.021

24. Hasegawa A, Yoshida K, Asano Y, Okada T, Iinuma T, Ito Y (2012) Change in stress field after the 2011 great Tohoku-Oki earthquake, Earth Planet. Sci Lett 355–356:231–243. doi:10.1016/j.epsl.2012.08.042

25. Iinuma T, Hino R, Kido M, Inazu D, Osada Y, Ito Y, Ohzono M, Tsushima H, Suzuki S, Fujimoto H, Miura S (2012) Coseismic slip distribution of the 2011 off the Pacific coast of Tohoku earthquake (M9.0) refined by means of seafloor geodetic data. J Geophys Res 117:B07409, 10.1029/2012JB009186

26. Romano F, Piatanesi A, Lorito S, D'Agostino N, Hirata K, Atzori S, Yamazaki Y, Cocco M (2012) Clues from joint inversion of tsunami and geodetic data of the 2011 Tohoku earthquake. Sci Rep 2:385. doi:10.1038/srep00385

27. Miura S, Takahashi N, Nakanishi A, Tsuru T, Kodaira S, Kaneda Y (2005) Structural characteristics off Miyagi forearc region, the Japan Trench seismogenic zone, deduced from a wide-angle reflection and refraction study. Tectonophysics 407:165–188

28. Tsuru T, Park J-O, Miura S, Kodaira S, Kido Y, Hayashi T (2002) Along-arc structural variation of the plate boundary at the Japan Trench margin: implication of interpolate coupling. J Geophys Res 107:2,357. doi:10.1029/2001JB001664

29. Michael AJ (1987) Use of focal mechanisms to determine stress: a control study. J Geophys Res 92:357–368. doi:10.1029/JB092iB01p00357

30. Chiba K, Iio Y, Fukahata Y (2012) Detailed stress fields in the focal region of the 2011 off the Pacific coast of Tohoku earthquake—implication for the distribution of moment release. Earth Planets Space 64(12):1157–1165. doi:10.5047/eps.2012.07.008

31. Lay T, Duputel Z, Ye L, Kanamori H (2013) The December 7, 2012 Japan Trench intraplate doublet (Mw 7.2, 7.1) and interactions between near-trench intraplate thrust and normal faulting. Phys Earth Planet Int 220:73–78. doi:10.1016/j.pepi.2013.04.009

32. Seno T, Yamanaka Y (1996) Double seismic zones, compressional deep trench-outer rise events and superplumes. In: Bebout GE et al (eds) Subduction: top to bottom, vol 96, Geophys. Monograph Ser. AGU, Washington, D.C., pp 347–355

33. Gamage SSN, Umino N, Hasegawa A, Kirby SH (2009) Offshore double-planed shallow seismic zone in the NE Japan forearc region revealed by sP depth phases recorded by regional networks. Geophys J Int 178:195–214. doi:10.1111/j.1365-246X.2009.04048.x

34. Romano F, Trasatti E, Lorito S, Piromallo C, Piatanesi A, Ito Y, Zhao D, Hirata K, Lanucara P, Cocco M (2014) Structural control on the Tohoku earthquake rupture process investigated by 3D FEM, tsunami and geodetic data. Sci Rep 4:5631. doi:10.1038/srep05631

35. DeMets C, Gordon RG, Argus DF, Stein S (1994) Effect of recent revisions to the geomagnetic reversal time scale on estimates of current plate motions. Geophys Res Lett 21:2192–2194

36. Sella GF, Dixon H, Mao A (2002) REVEL: a model for recent plate velocities from space geodesy. J Geophys Res 107(B4):2081. doi:10.1029/2000JB000033

37. Yamanaka Y, Kikuchi M (2004) Asperity map along the subduction zones in NE Japan inferred from regional seismic data. J Geophys Res 109, B07307. doi:10.1029/2003JB002683

38. Murotani S, Kikuchi M, Yamanaka Y, Shimazaki K (2004) Rupture process of large Fukushima-Oki earthquakes (2). Seism. Soc. of Japan (SSJ), Fall Meeting, Hakozaki, Japan, p P029

39. Ohta Y, Hino R, Inazu D, Ohzono M, Ito Y, Mishina M, Iinuma T, Nakajima J, Osada Y, Suzuki K, Fujimoto H, Tachibana K, Demachi T, Miura S (2012) Geodetic constraints on afterslip characteristics following the March 9, 2011, Sanriku-oki earthquake, Japan. Geophys Res Lett 39:L16304. doi:10.1029/2012GL052430

40. Hino R, Inazu D, Ohta Y, Ito Y, Suzuki S, Iinuma T, Osada Y, Kido M, Fujimoto H, and Kaneda Y (2013). Was the 2011 Tohoku-Oki earthquake preceded by aseismic preslip? Examination of seafloor vertical deformation data near the epicenter. Mar. Geophys. Res. doi: 10.1007/s11001-013-9208-2

41. Zhao D, Huang Z, Umino N, Hasegawa A, Kanamori H (2011) Structural heterogeneity in the megathrust zone and mechanism of the 2011 Tohoku-Oki earthquake (Mw 9.0). Geophys Res Lett 38:L17308, doi:10.1029/2011GL048408

42. Eberhart-Phillips D and Michael AJ (1993) Three-dimensional velocity structure, seismicity, and fault structure in the Parkfield Region, Central California. J Geophys Res. 98. doi:10.1029/93JB01029, issn: 0148–0227.

43. Okada T, Hasegawa A, Suganomata J, Zhao D, Zhang H, Thurber C (2006) Imaging the source area of the 1995 southern Hyogo (Kobe) earthquake (M7.3) using double-difference tomography. Earth Planet Sci Lett 253:143–150

44. Okada T, Yaginuma T, Umino N, Matsuzawa T, Hasegawa A, Zhang H, Thurber CH (2006) Detailed imaging of the fault planes of the 2004 Niigata-Chuetsu, central Japan, earthquake sequence by double-difference tomography. Earth Planet Sci Lett 244:32–43

45. Yamamoto Y, Obana K, Kodaira S, Hino R, Shinohara M (2013) Structural heterogeneities around the megathrust zone of the 2011 Tohoku earthquake from tomographic inversion of onshore and offshore seismic observations. J Geophys Res 119:1165–1180. doi:10.1002/2013JB010582